



University of Dundee

Mechanisms of hydrogen sulfide removal by ground granulated blast furnace slag amended soil

Xie, Mengyao; Leung, Anthony Kwan; Ng, Charles Wang Wai

Published in:
Chemosphere

DOI:
[10.1016/j.chemosphere.2017.02.016](https://doi.org/10.1016/j.chemosphere.2017.02.016)

Publication date:
2017

Document Version
Peer reviewed version

[Link to publication in Discovery Research Portal](#)

Citation for published version (APA):

Xie, M., Leung, A. K., & Ng, C. W. W. (2017). Mechanisms of hydrogen sulfide removal by ground granulated blast furnace slag amended soil. *Chemosphere*, 175, 425-430.
<https://doi.org/10.1016/j.chemosphere.2017.02.016>

General rights

Copyright and moral rights for the publications made accessible in Discovery Research Portal are retained by the authors and/or other copyright owners and it is a condition of accessing publications that users recognise and abide by the legal requirements associated with these rights.

- Users may download and print one copy of any publication from Discovery Research Portal for the purpose of private study or research.
- You may not further distribute the material or use it for any profit-making activity or commercial gain.
- You may freely distribute the URL identifying the publication in the public portal.

Take down policy

If you believe that this document breaches copyright please contact us providing details, and we will remove access to the work immediately and investigate your claim.

1 **Mechanisms of hydrogen sulfide removal by ground granulated blast furnace slag amended soil**

2

3 Mengyao Xie¹; Anthony Kwan Leung²; Charles Wang Wai Ng³

4

5 ¹Department of Civil and Environmental Engineering, Hong Kong University of Science and
6 Technology, Clear Water Bay, Kowloon, Hong Kong (corresponding author). Email:

7 mxieac@connect.ust.hk

8

9 ²Division of Civil Engineering, University of Dundee, DD1 4HN, United Kingdom. Email:

10 a.leung@dundee.ac.uk

11

12 ³Department of Civil and Environmental Engineering, Hong Kong University of Science and
13 Technology, Clear Water Bay, Kowloon, Hong Kong. Email: cecwwng@ust.hk

14

15 Abstract

16 Ground granulated blast furnace slag (GGBS) amended soil has been found able to remove

17 gaseous hydrogen sulfide (H₂S). However, how H₂S is removed by GGBS amended soil and

18 why GGBS amended soil can be regenerated to remove H₂S are not fully understood. In this

19 study, laboratory column tests together with chemical analysis were conducted to investigate

20 and reveal the mechanisms of H₂S removal process in GGBS amended soil. Sulfur products

21 formed on the surface of soil particle and in pore water were quantified. The test results

22 reveal that the reaction between H₂S and GGBS amended soil was combined process of

23 oxidation and acid-base reaction. The principal mechanism to remove H₂S in GGBS amended

24 soil was through the formation of acid volatile sulfide (AVS), elemental sulfur and

25 thiosulfate. Soil pH value decreased gradually during regeneration and reuse cycles. It is

26 found that the AVS plays a significant role in H₂S removal during regeneration and reuse
27 cycles. Adding GGBS increased the production of AVS and at the same time suppressed the
28 formation of elemental sulfur. This mechanism is found to be more prominent when the soil
29 water content is higher, leading to increased removal capacity.

30

31 Keywords

32 H₂S, GGBS, sulfur, AVS, regeneration

33

34 1. Introduction

35 Ground granulated blast furnace slag (GGBS) is a by-product of iron and steel industry.
36 Large amounts of GGBS are generated each year (e.g., production capacity of 10 million tons,
37 “K. Wah Construction Material,” 2016). GGBS is rich in minerals, finely granulated and
38 highly alkaline. Its most popular use is to replace cement in concrete to improve strength,
39 durability, decrease permeability and retard setting (Oner and Akyuz, 2007). GGBS has also
40 be sometimes used for soil solidification and stabilization (Kogbara and Al-Tabbaa, 2011).

41

42 Landfill is a source of odorous gas, mainly in the form of H₂S. The odorous gas would
43 migrate through landfill cover soil and cause serious environmental problems. GGBS has
44 been shown to be an effective soil conditioner to reduce H₂S concentration (Ng et al., 2016).
45 The laboratory study shows that GGBS amended soil could reduce H₂S to a level lower than
46 the olfactory threshold of 0.02 ppm (i.e., the lowest H₂S concentration that human nose could
47 sense), and it can be regenerated multiple times to maintain its removal capacity. The
48 mechanisms involved in H₂S removal and its regeneration/reuse are, however, unclear.
49 Factors that control the capacity of GGBS for H₂S removal are not known.

50

51 Linz-Donawitz Steel Slag (LD) and Steel Making Slag (SMS), which have similar
52 composition with GGBS, have been also found effective in removal of H₂S (Kim et al., 2012;
53 Montes-Morán et al., 2012). The existing studies show that elemental sulfur S(0) can be
54 found as a product of the LD-H₂S reaction. Kim et al (2012) estimated sulfur transformation
55 during the removal of aqueous H₂S by SMS and found that the major products were S(0) and
56 manganese sulfide (MnS). Sulfur transformation in unsaturated soil condition (which is often
57 the case for a landfill cover), on the other hand, would be substantially different because soil
58 water content may play a major role. This is because water could influence the physical state
59 of reactant (e.g., gaseous or aqueous), hence the reaction kinetics.

60

61 The objective of this paper is to quantify the sulfur transformation and phase transfer upon
62 H₂S removal by GGBS amended unsaturated soil. Sulfur products in soil samples before/after
63 reaction and during each regeneration/reuse cycles were measured. Influences of soil water
64 content on the removal mechanisms are then investigated.

65

66 2. Materials and methods

67 2.1 Material properties

68 Loess soil (silty clay) was collected from Xi'an, China. GGBS was provided by K. Wah
69 Construction Company, Hong Kong. Loess soil samples were amended with 0% and 30% (by
70 mass) GGBS. pH values of loess and GGBS are 8.36 and 11.67, respectively. pH value of
71 loess amended with 30% GGBS is 11.74. Measurements show that after adding 30% GGBS
72 (mean particle size of GGBS is 9.33 μm), the mean particle size of amended soil shifts from
73 35.36 μm to 27.87 μm. Metal contents of loess soil and GGBS were obtained using X-ray
74 fluorescence (XRF), and they are summarized in Table 1. Chemico-physical properties of

75 loess, GGBS and their mixtures were measured and are listed in Table 2. Water used in all
76 the tests in this study was ultrapure water. Chemicals were provided by Sigma-Aldrich.

77

78 2.2 Sample preparation and analysis methods

79 Dynamic H₂S removal tests and regeneration tests were carried out. Loess soil was amended
80 with 0% and 30% GGBS, compacted to the same bulk density (1.54 g/cm³) in a soil column.

81 A concentration of 1000 ppm H₂S was supplied from the bottom of each column at a constant
82 rate of 50 mL/min. The tests would stop when H₂S breakthrough took place. H₂S

83 breakthrough is defined when the H₂S concentration at the column outlet reached the

84 olfactory threshold of 0.02 ppm. H₂S removal capacity is defined as the maximum sulfur

85 (sulfur in H₂S, unit mg) that can be removed by 1 g of soil (bulk mass) before H₂S

86 breakthrough. Regeneration method was air ventilation. Detailed test procedures are reported

87 by (Ng et al., 2016). In order to investigate the effects of soil water content on H₂S removal

88 capacity and removal mechanisms, GGBS amended soils with different gravimetric water

89 contents (i.e., 0%, 10% and 20%) were tested. For the GGBS amended soil with water

90 content of 20%, three regeneration and reuse cycles were applied. The testing program is

91 shown in Table 3.

92

93 After each column test, two soil samples (around 4 g each) were collected from the lower part

94 of the soil column. These two samples were placed into two separate 250 ml pyrex glass

95 bottles, namely A and B. Bottle A was used for the measurements of the concentration of

96 soluble sulfide, sulfate and thiosulfate in soil water, while bottle B was used to measure the

97 concentration of elemental sulfur S(0) and acid volatile sulfide (AVS) on soil particle.

98 Detailed measurement procedures of these chemicals are given in the next section. Both

99 bottles A and B contained 30 ml of ultrapure water and 5 drops of 10 N sodium hydroxide

100 (NaOH), aiming to increase the pH to prevent sulfide ion from forming H₂S. Soil in the bottle
101 A was agitated by magnetic stirrers to facilitate soluble sulfide, sulfate and thiosulfate to
102 dissolve in the water. After agitation, the soil-water mixture was allowed to stand and
103 segregate. A flow chart of chemical measurements can be found in Fig. S1 in the
104 supplementary information (SI). Each condition was tested for two replicates.

105

106 2.2.1 Measurements of soluble sulfide, sulfate and thiosulfate in soil pore water

107 Supernatant from the bottle A was filtered through 0.45 µm filter (Sartorius Stedim), and the
108 filtrate was collected. The filtrate was firstly taken for measuring the concentration of soluble
109 sulfide using the methylene blue method (APHA, 2005). In this method: 1 drop of 10N
110 NaOH was added into 6 ml filtrate sample, and then 0.4 ml amine sulfuric acid and 0.12 ml
111 ferric chloride (FeCl₃) solution were added to filtrate sample. The filtrate was mixed and
112 stood for 5 min, and then 1.28 ml diammonium hydrogen phosphate solution was added to
113 the filtrated sample. Subsequently the sample stood for 20 min to let precipitates to settle
114 down, and then the supernatant was collected and measured with methylene blue absorbance
115 at 664 nm using a UV/Vis spectrophotometer (Lambda 25, Perkin Elmer Inc., USA) with a
116 cuvette providing a light path of 10 mm, and a sulfide measuring range of 0 to 1 mg/L.

117

118 5 ml filtrate from the bottle A was also collected and added with a drop of 1 N zinc acetate
119 (Zn(Ac)₂) and a drop of 6N NaOH, and it was mixed and allowed to stand for 10 min for the
120 precipitates of ZnS to settle). Then the supernatant was filtered through 0.45 µm filter again,
121 and the filtrate was used for the measurements of soluble sulfate and thiosulfate, by an ion
122 chromatograph (100, Dionex, USA) equipped with a conductivity detector and an IonPac
123 AS9-HC analytical column.

124

125 2.2.2 Measurements of insoluble AVS, elemental sulfur S(0) on soil particle surface

126 Measurements of AVS were performed by acidifying samples (USEPA, 1991). Bottle B was
127 firstly purged with nitrogen gas (N₂). Then 20 ml concentrated hydrogen chloride (HCl) was
128 added to the soil sample, followed by agitating using a magnetic stirrer. Gas generated from
129 the acid-treated soil was stripped into two serial traps filled with 1 N NaOH solution. After
130 the acid treatment, N₂ gas was injected into the acid-treated soil for one hour continuously to
131 remove any remaining H₂S. Details of the testing apparatus are provided in Fig. S2 in the SI.
132 After an hour of N₂ injection, H₂S absorbed in the NaOH solution was quantified using the
133 methylene blue method (APHA, 2005). The amount of sulfide available in AVS was obtained
134 by subtracting the concentration of soluble sulfide obtained from the previous step (section
135 2.2.1) from the concentration of sulfide measured in this procedure.

136

137 S(0) in the soil samples was measured by the revised method suggested by McGuire and
138 Hamers (2000). After the acid treatment and one hour of N₂ purging, the sealed bottle B was
139 added with 20 ml Tetrachloroethylene (C₂Cl₄), and then shaken continuously for four hours
140 in a spinning shaker. Subsequently, C₂Cl₄, which carried extracted S(0), was collected and
141 filtered through 0.2 μm membrane (Sigma-Aldrich). S(0) was measured using a high
142 performance liquid chromatography (HPLC, LC-30AD, Shimadzu, Japan) equipped with a
143 Waters symmetry C18 column (4.6 mm × 150 mm, 5 μm particle size) and a UV detector set
144 at 254 nm. An eluent of 90% acetonitrile + 10% water was used at a flow rate of 1 mL/min.

145

146 It should be noted that any thiosulfate available in the bottle B would turn into sulfur dioxide
147 (SO₂) and S(0) once the soil was treated with concentrated HCl (see Equation [1]). Therefore,
148 in order to analyze S(0) produced during H₂S removal, it is required to subtract S(0)
149 generated from thiosulfate from that measured by HPLC.

150



151

152 Soil samples were collected from each soil column for chemico-physical characterizations.
153 pH measurement was carried out according to the standard ASTM D4972-13 (ASTM, 2001)
154 using a pH meter (Oakton Instruments). Surface elements were identified by an X-ray
155 photoelectron spectroscopy (XPS, Axis Ultra DLD model). Microstructure was investigated
156 using a Scanning electron microscope (SEM, JSM 6300 (JEOL) model).

157

158 3. Results and discussions

159 In this study, the initial sulfur components of soil samples before reacting with H₂S were
160 measured. Therefore, for the results presented herein, all sulfur products refer to the net sulfur
161 product formed by H₂S reaction.

162

163 The major sulfur products in the soil during reaction, regeneration and reuse were identified
164 by the XPS spectrum (see Fig. S3 in the SI). According to the XPS spectra data of sulfur
165 species reported by Moulder (1992), the peaks of mineral sulfide, elemental sulfur,
166 thiosulfate and sulfate could be identified in a S(2p) XPS spectra at binding energies of 162.6
167 eV, 164 eV, 167.8 eV and 168.8 eV (see x-axis in Fig. S3), respectively. Therefore, the major
168 reaction products of H₂S removal by the GGBS amended soil were metal sulfide, elemental
169 sulfur, thiosulfate and sulfate. This suggests that the chemical analysis were able to cover
170 most of the reaction products.

171

172 Fig. 1 shows that for LH and L30GH, H₂S input is almost equal to the sum of all the
173 measured sulfur products. This means that the mass balance of sulfur was almost achieved,
174 and most of the sulfur products have been captured in these tests. For LH, almost all H₂S was
175 transferred into elemental sulfur, S(0). This was attributable to the oxidation of H₂S by the
176 minerals available in loess. For L30GH, H₂S was transferred into 68% AVS, 13% S(0), 11%
177 thiosulfate and 6% sulfide. It was found that the form of H₂S present in soil was controlled by
178 the pH value (Haimour et al., 2005; He et al., 2011). S²⁻ is dominant when pH value is higher
179 than 10. On the contrary, when pH is between 8 and 9, HS⁻ is dominant, whereas no S²⁻
180 exists in solution for any pH lower than 8. Since the pH value of L is 8.36 (Table 2), HS⁻ was
181 likely to be the main form of H₂S existed in soil. As shown in Fig. 1, H₂S in the sample LH
182 was mainly oxidized into S(0), and very few sulfide was found. On the other hand, pH value
183 of the soil sample L30G was 11.74 (Table 2), so it is not surprising to find more sulfide in the
184 soil sample. This is similar to LD slag that its strong alkalinity would trigger dissociation of
185 dissolved H₂S into S²⁻ and HS⁻ (Montes-Morán et al., 2012). The results also show that
186 adding GGBS could suppress the formation of S(0). This seems to indicate that the use of
187 GGBS may be beneficial for improving the H₂S removal capacity in regeneration cycles
188 because precipitation of S(0) on the surface of soil particles could block the reactive sites
189 substantially (Sun et al., 2014). Moreover, adding GGBS to soil increased the production of
190 AVS, probably because of the higher mineral content in GGBS (Table 1) and increased
191 surface activity due to its high alkalinity. The significance of having high AVS production is
192 discussed later.

193

194 Fig. 2 (A) shows that sulfide ions decreased during regeneration, and increased during reuse.
195 This was because of the dissolution of H₂S in pore water during the reuse, and the oxidation
196 of sulfide by O₂ during regeneration, according to the following chemical Equation [2].

197



198 (Chen and Morris, 1972; Davydov et al., 1998)

199

200 It should be noted that sulfide would be oxidized into different products when supplying
201 different amount of O₂, as indicated in Equation [2]. Although the formation of thiosulfate,
202 sulfate and elemental sulfur through sulfide oxidation also contributed to the overall sulfur
203 transformation, this was only at very small scale because the total sulfide in pore water was
204 low (<0.06 mg/g).

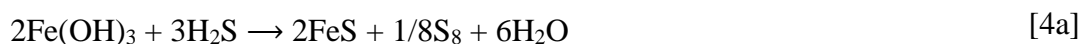
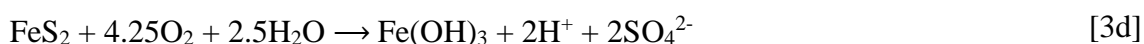
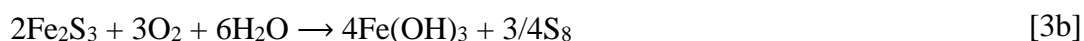
205

206 Fig. 2 (B) shows that AVS decreased during regeneration, and increased during reuse.

207 Previous studies show that some AVS were very sensitive to O₂. For instance, any exposure
208 of AVS to O₂ would change the nature of some potential AVS minerals such as mackinawite
209 and greigite (Rickard and Morse, 2005). Possible mechanisms are given in Equations [3-4]
210 (which use iron mineral as an example; other minerals may apply). It can be seen from Fig. 2
211 (B) that although AVS changed during several regeneration and reuse, its content was within
212 a relatively constant range between 0.3 mg/g – 0.6 mg/g. This may be because part of the
213 AVS acted as a catalyst to remove H₂S (see Equation [3-4]). During regeneration, AVS
214 turned into mineral oxide/hydroxide (e.g., Fe(OH)₃), as shown in Equation [3a-d]. While
215 during reuse, mineral oxides/hydroxide reacted with H₂S and AVS was formed again, as
216 shown in Equation [4a-d]. This is the reason why GGBS amended soil could be regenerated
217 to remove H₂S through air ventilation. This is similar to the mechanism when Linz-Donawitz
218 Steel Slag is used to remove H₂S, the reaction during which the transition metal oxides and/or

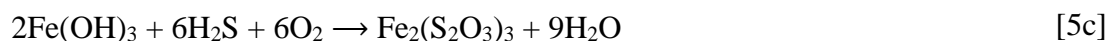
219 hydroxides would act as active catalysts to oxidize H₂S to elemental sulfur (Montes-Morán et
220 al., 2012). It should be noted that for Equations [3a-c] and [4a], during both regeneration and
221 reuse, S(0) would be formed, and this may be the reason that caused continuous increase in
222 S(0) from L30GH to R3 (see Fig. 2 (B)).

223



224 (Davydov et al., 1998; Schippers and Jorgensen, 2002).

225



226 (Cantrell et al., 2003)

227

228 In Fig. 2 (A), the measured increase in sulfate ion during regeneration is likely to be
229 attributable to the oxidation of pyrite (Equation [3d]), as well as the oxidation of sulfide
230 (Equation [2b]). Biological oxidation of other reduced sulfur products might be another
231 reason that caused the increase in sulfate through R2 to R3. Sulfur oxidizing bacteria (SOB)

232 would use the energy of reduced sulfur compounds (e.g., H₂S, thiosulfates, sulfites, and
233 elemental sulfur), and then convert the reduced sulfur compounds to sulfate. The optimum
234 pH values for SOB growth are typically between 1 and 9 (Pokorna and Zabranska, 2015). As
235 can be seen in Fig. 3, during regeneration and reuse cycles, the pH value showed a decreasing
236 trend from about 12 to 9. Thus, it is likely that SOB has been activated and produced sulfate
237 through biological oxidation. The observed pH drop in Fig. 3 was attributable to the
238 dissolution of H₂S during reuse, and oxidation of sulfide ion and pyrite during regeneration.
239 As indicated in Equation [2b] and [3d], both processes would produce hydrogen ion, hence
240 results in decrease of pH value. At R3, the pH value was still around 9, indicating that HS⁻
241 and S²⁻ both existed and they were stable in the pore water.

242

243 On the other hand, the observed increase in thiosulfate during both regeneration (except for
244 R2) and reuse (see Fig. 2 (B)) is likely to be the consequence of the oxidation of sulfide
245 (Equation [2a]) and the aerobic reaction between mineral hydroxide and H₂S during reuse
246 (Equation [5c]). Since oxygen might dissolve in pore water during regeneration, aerobic
247 reactions might have taken place between H₂S and the soil, hence leading to the production
248 of sulfate and thiosulfate during reuse. When comparing the reaction products from initial
249 H₂S removal (i.e., L30GH) and the removal after regeneration (i.e., R1H and R2H), it
250 demonstrates that there was a change in removal mechanism. For the initial H₂S removal, the
251 main reaction product was AVS (Fig. 1), indicating that most H₂S was bonded with the
252 minerals in the soil. For H₂S removal in the subsequent regenerated cycles, S(0) was
253 accumulated while AVS remained at 0.3 mg/g – 0.6 mg/g (Fig. 2 (B)). This indicates that
254 during regeneration/reuse cycles, the major removal mechanism of H₂S was through the
255 oxidization to S(0).

256

257 SEM images depicted in Fig. 4 show that for R3 (where most sulfur products were found
258 compared to others), needle-like elemental sulfur crystal could be identified and it spreads
259 around the surface of soil particles. Small amount of octahedral pyrite can also be seen. This
260 further confirms the proposed removal mechanisms discussed in Equation [3], [4] and [5].
261 Moreover, because the metal hydroxide/oxide generated from oxidation of AVS acted as a
262 catalyst during the removal of H₂S, the H₂S removal capacity would not change much during
263 each reuse cycle due to relatively constant range of AVS (Fig. 2 (B)). However, precipitation
264 of elemental sulfur on particle surface would gradually reduce the availability of reactive
265 sites and hinder further regeneration and reuse (Sun et al., 2014). Therefore, the H₂S removal
266 capacity was gradually reduced at the subsequent regeneration/reuse cycles (Ng et al., 2016).
267

268 Fig. 5 shows the effects of different soil water contents on the removal capacity and removal
269 mechanisms. The removal capacity increased with an increase in soil water content from 0%
270 to 20%. This appears to agree with the findings reported by Montes-Morán et al (2012) who
271 showed that the relative humidity of the slags particles changed dramatically with the H₂S
272 removal capacity. The water solubility of H₂S is relatively high: 7100 mg/L at 0 °C, and 3925
273 mg/L at 20 °C (Bergersen and Haarstad, 2008). Therefore, higher soil water content would
274 result in more H₂S dissolving in the pore water, and hence more H₂S could be removed from
275 its gas phase. Also, for a given soil dry density, increasing soil water content would decrease
276 the pore air ratio. This would hence (i) reduce the effective diffusion coefficient, and
277 therefore more effectively limit H₂S migration and (ii) extend the retention time of H₂S in the
278 soil, resulting in a higher H₂S removal capacity (Xu et al., 2014). Moreover, it can be seen in
279 Fig. 5 that higher soil water content facilitated AVS formation and suppressed the formation
280 of elemental sulfur. The AVS content increased from 0.166 to 0.527 mg/g (in percentage:
281 from 36% to 68%), while the elemental sulfur decreased from 0.259 to 0.0988 mg/g (from

282 56% to 13%). Since AVS plays an important role in H₂S removal during regeneration/reuse
283 cycles (see Fig. 2 (B)), increasing AVS content by increasing soil water content is likely to be
284 able to improve H₂S removal capacity during regeneration. Because the accumulation of
285 elemental sulfur would block the availability of reactive sites on the surface of soil particle,
286 reducing elemental sulfur production by increasing soil water content may also improve H₂S
287 removal capacity in regeneration cycles. The test results imply that GGBS amended soil
288 would be suitable to be used as in a landfill cover located in humid regions, because the
289 increase in soil water content due to rainfall could improve the H₂S removal capacity for not
290 only the initial removal but also probably the removal in the subsequent regeneration/reuse
291 cycles.

292

293 In Figs 5 and 6, it can be seen that for the first two regeneration cycles of the sample with
294 20% of soil water content (i.e., from L30GH to R2 in Fig. 6), the removal capacities were
295 almost equal to the sum of the measured sulfur products. For the third regeneration cycle of
296 the samples (i.e., R2H and R3 in Fig. 6) and samples with lower water content (i.e., 0% and
297 10% in Fig. 5), however, the sum of the measured sulfur products were higher than the
298 removal capacities. This inconsistency may be associated with the reduction of reaction
299 kinetics between H₂S and those samples. It was demonstrated by Xu et al (2014) that in a
300 diffusion-advection-reaction system, any change of reaction kinetics could affect the
301 distribution of H₂S in a soil bed. Hence, a non-uniform distribution of sulfur products along
302 the soil column would be resulted, where the lower part would contain higher sulfur products,
303 whereas the higher part contains less. Since the soil samples tested in the present study were
304 taken at the lower part of the soil columns, their sulfur products content would be higher than
305 the average sulfur content calculated from H₂S input.

306

307 4. Conclusions

308 This study presents a set of comprehensive laboratory testing that provides insights into the
309 pathways and mechanisms of how H₂S would be removed by GGBS amended soil. The test
310 results show that gaseous H₂S could be removed by the GGBS in soil through oxidation and
311 acid-base combined reactions. Using GGBS to react with H₂S caused an increase production
312 of acid volatile sulfide (AVS) and suppressed the formation of elemental sulfur. AVS has
313 shown to play an important role in H₂S removal during regeneration and reuse cycles. Soil
314 pH value gradually decreased during regeneration and reuse cycles. Precipitation of
315 elemental sulfur on particle surface was unfavorable for H₂S removal. Increasing water
316 content of GGBS amended soil up to a 20% (by weight) is favorable for H₂S removal
317 because this promoted H₂S dissolution, simultaneously facilitating the formation of AVS and
318 suppressing the formation of elemental sulfur.

319

320 Acknowledgements

321 The authors would like to acknowledge the research grant grant (HKUST6/CRF/12R)
322 provided by the Research Grants Council (RGC) of the Hong Kong Special Administrative
323 Region. The second author would also like to acknowledge the research travel support from
324 the Northern Research Partnership (NRP).

325

326 References

327 APHA, 2005. Standard methods for the examination of water and wastewater. Washington,
328 DC, USA.

329 ASTM, I., 2001. Standart Test Method for pH of Soils. ASTM D4972 - 01. ASTM Stand.

330 Test 1, 1–5. doi:10.1520/D4972-01R07.2

331 Bergersen, O., Haarstad, K., 2008. Metal oxides remove hydrogen sulfide from landfill gas

332 produced from waste mixed with plaster board under wet conditions. *J. Air Waste*
333 *Manage. Assoc.* 58, 1014–1021. doi:10.3155/1047-3289.58.8.1014

334 Cantrell, K.J., Yabusaki, S.B., Engelhard, M.H., Mitroshkov, A. V., Thornton, E.C., 2003.
335 Oxidation of H₂S by iron oxides in unsaturated conditions. *Environ. Sci. Technol.* 37,
336 2192–2199. doi:10.1021/es020994o

337 Chen, K., Morris, J., 1972. Kinetics of Oxidation of Aqueous Sulfide by O₂. *Environ. Sci.*
338 *Technol.* 6, 529–537. doi:10.1021/es60065a008

339 Davydov, A., Chuang, K.K.T., Sanger, A.A.R., 1998. Mechanism of H₂S oxidation by ferric
340 oxide and hydroxide surfaces. *J. Phys. Chem.* 102, 4745–4752.

341 Haimour, N., El-Bishtawi, R., Ail-Wahbi, A., 2005. Equilibrium adsorption of hydrogen
342 sulfide onto CuO and ZnO. *Desalination* 181, 145–152. doi:10.1016/j.desal.2005.02.017

343 He, R., Xia, F.F., Wang, J., Pan, C.L., Fang, C.R., 2011. Characterization of adsorption
344 removal of hydrogen sulfide by waste biocover soil, an alternative landfill cover. *J.*
345 *Hazard. Mater.* 186, 773–778. doi:10.1016/j.jhazmat.2010.11.062

346 K. Wah Construction Material, 2016. URL <http://www.kwcml.com/en/slag.php>

347 Kim, K., Asaoka, S., Yamamoto, T., Hayakawa, S., Takeda, K., Katayama, M., Onoue, T.,
348 2012. Mechanisms of hydrogen sulfide removal with steel making slag. *Environ. Sci.*
349 *Technol.* 46, 10169–10174. doi:10.1021/es301575u

350 Kogbara, R.B., Al-Tabbaa, A., 2011. Mechanical and leaching behaviour of slag-cement and
351 lime-activated slag stabilised/solidified contaminated soil. *Sci. Total Environ.* 409,
352 2325–2335. doi:10.1016/j.scitotenv.2011.02.037

353 McGuire, M., Hamers, R.J., 2000. Extraction and quantitative analysis of elemental sulfur
354 from sulfide mineral surfaces by high performance liquid chromatography 34, 4651–
355 4655.

356 Montes-Morán, M.A., Concheso, A., Canals-Batlle, C., Aguirre, N. V, Ania, C.O., Martín,

357 M.J., Masaguer, V., 2012. Linz-Donawitz Steel Slag for the Removal of Hydrogen
358 Sulfide at Room Temperature. *Environ. Sci. Technol.* 46, 8992–8997.
359 doi:10.1021/es301257c

360 Moulder, J.F., 1992. *Handbook of X-ray Photoelectron Spectroscopy: A Reference Book of*
361 *Standard Spectra for Identification and Interpretation of XPS Data*, illustrate. ed.
362 Physical Electronics Division, Perkin-Elmer Corporation.

363 Ng, C.W.W., Xie, M., Leung, A.K., 2016. Removal of hydrogen sulfide using soil amended
364 with ground granulated blast furnace. *J. Environ. Eng. ASCE* (In press).

365 Oner, A., Akyuz, S., 2007. An experimental study on optimum usage of GGBS for the
366 compressive strength of concrete. *Cem. Concr. Compos.* 29, 505–514.
367 doi:10.1016/j.cemconcomp.2007.01.001

368 Pokorna, D., Zabranska, J., 2015. Sulfur-oxidizing bacteria in environmental technology.
369 *Biotechnol. Adv.* 33, 1246–1259. doi:10.1016/j.biotechadv.2015.02.007

370 Rickard, D., Morse, J.W., 2005. Acid volatile sulfide (AVS), *Marine Chemistry*.
371 doi:10.1016/j.marchem.2005.08.004

372 Schippers, A., Jorgensen, B.B., 2002. Biogeochemistry of pyrite and iron sulfide oxidation in
373 marine sediments. *Geochim. Cosmochim. Acta* 66, 85–92. doi:10.1016/S0016-
374 7037(01)00745-1

375 Sun, J., Zhou, J., Shang, C., Kikkert, G.A., 2014. Removal of aqueous hydrogen sulfide by
376 granular ferric hydroxide-Kinetics, capacity and reuse. *Chemosphere* 117, 324–329.
377 doi:10.1016/j.chemosphere.2014.07.086

378 USEPA, 1991. *Draft Analytical Method for Determination of Acid Volatile Sulfide in*
379 *Sediment*. United States.

380 Xu, Q., Powell, J., Jain, P., Townsend, T., 2014. Modeling of H₂S migration through landfill
381 cover materials. *J. Hazard. Mater.* 264, 254–260. doi:10.1016/j.jhazmat.2013.11.005

382
383

Table 1. Metal content (weight percentage of dry matter) obtained from XRF analyses

Type	CaO	SiO ₂	Al ₂ O ₃	MgO	TiO ₂	K ₂ O	MnO	Fe ₂ O ₃
Loess	22.8	61.1	7.6	10.5	0.8	1.3	0.0	3.6
GGBS	37.9	34.2	13.8	8.1	1.0	0.6	0.5	0.3

384
385
386
387

Table 2. Properties of loess and amended loess tested in this study

Soil condition	ID	G _s (kg/m ³) ^a	pH value ^b	Mean particle size (μm) ^b	S _s (m ² /g)
Loess	L	2690	8.36	35.36	22.58
Loess+30% GGBS	L30G	2760	11.74	27.87	15.95
GGBS	-	2924	11.67	9.33	1.28

388 ^aG_s is specific gravity
389 ^b Mean value of three repeated tests
390

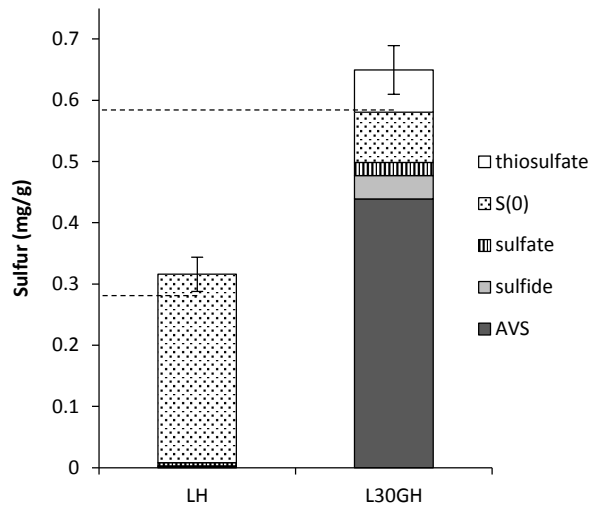
391

Table 3. Testing program

393
394

Soil condition	Water content	Regeneration cycle	Sample ID*	
			Before H ₂ S	After H ₂ S
Loess	15%	-	L	LH
Loess + 30%GGBS	20%	-	L30G	L30GH
		1	R1	R1H
		2	R2	R2H
Loess + 30%GGBS	20%	3	R3	-
		0%		
Loess + 30%GGBS	10%			
	20%			

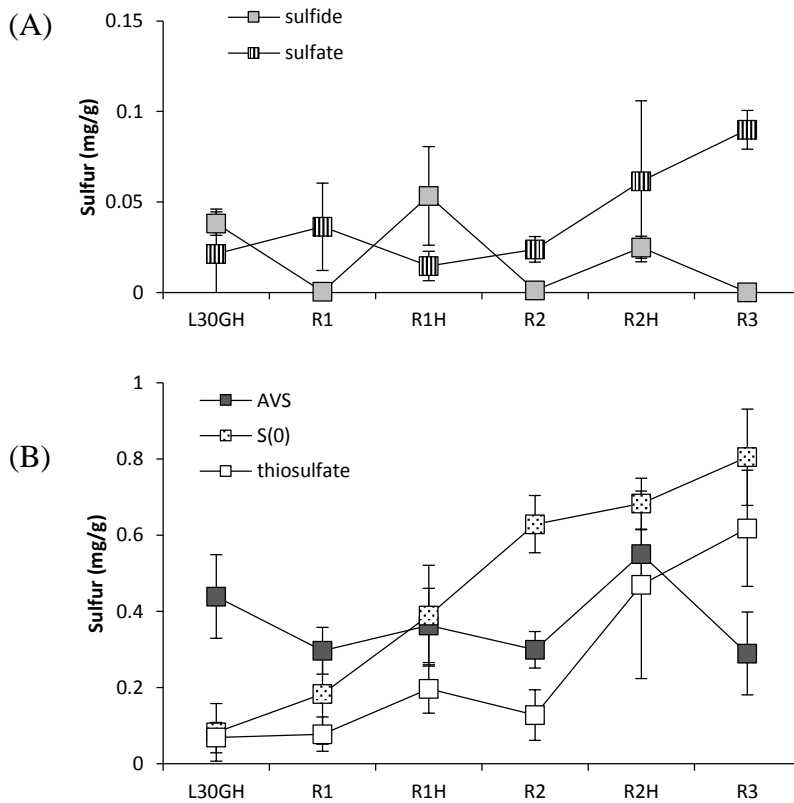
* RX is the soil sample after the Xth cycle of regeneration, RXH is the soil sample RX after reacting with H₂S. For example, R1 is the soil sample L30GH after the 1st cycle of regeneration. R1H is the soil sample R1 after reacting with H₂S. R2 is the soil sample R1H after the 2nd cycle of regeneration.



395
396
397

Fig. 1. Sulfur products in soil after reaction with H₂S. Dotted lines represent H₂S input calculated from column tests, error bars represent mean absolute deviation. Sulfur content in y-axis is expressed as mg of sulfur per 1 g of bulk soil.

398
399
400



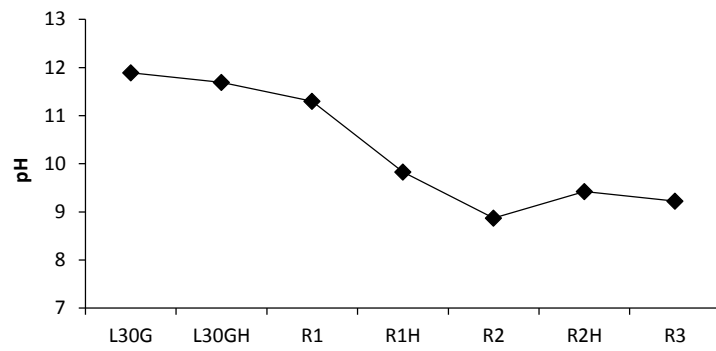
401
402

403
404
405
406
407

Fig. 2. Sulfur transformation in regeneration/reuse of L30G. Error bars represent mean absolute deviation. Sulfur content in y-axis is expressed as mg of sulfur per 1 g of bulk soil.

408

409
410
411



412
413

Fig. 3. pH value of L30G during regeneration and reuse

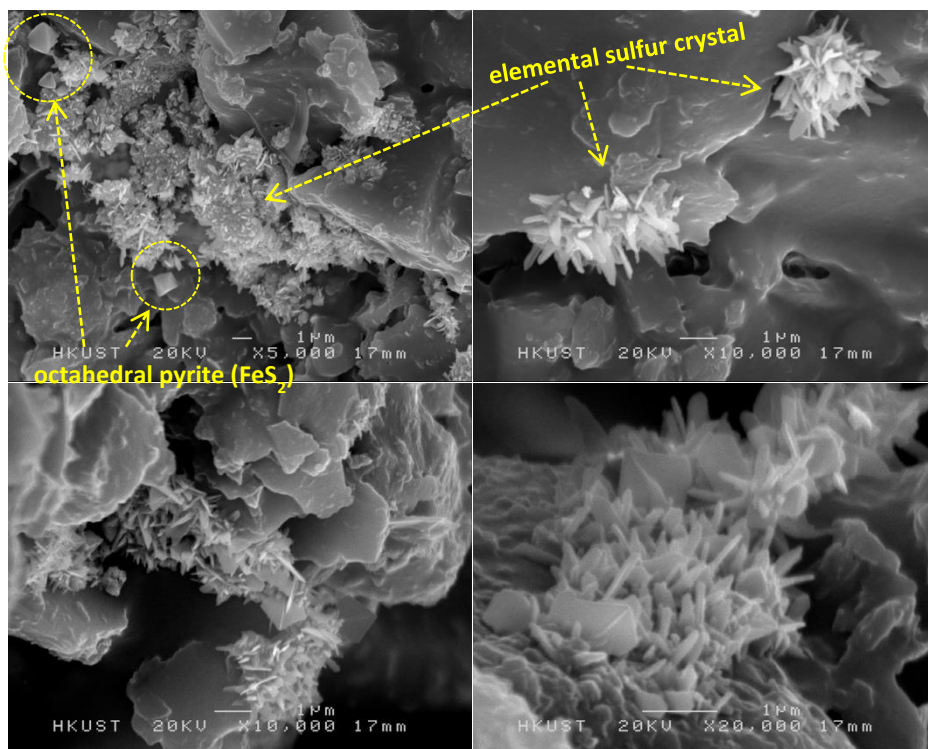
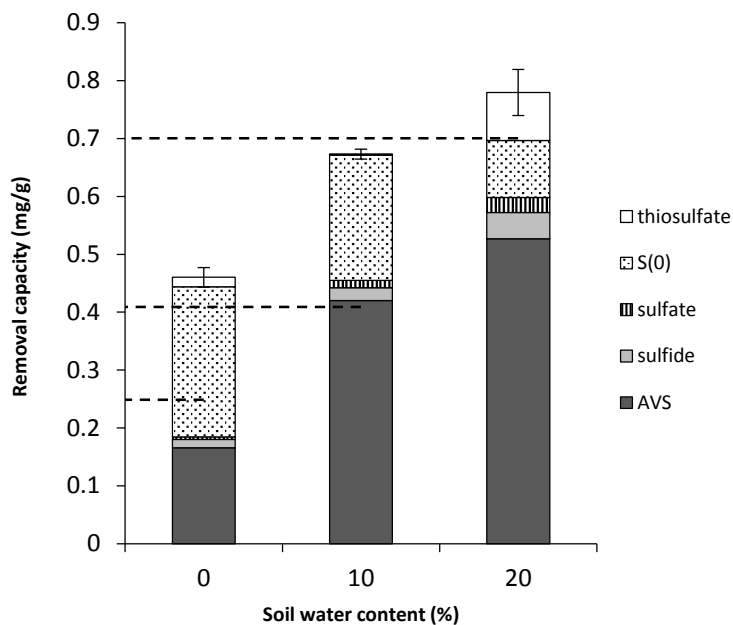


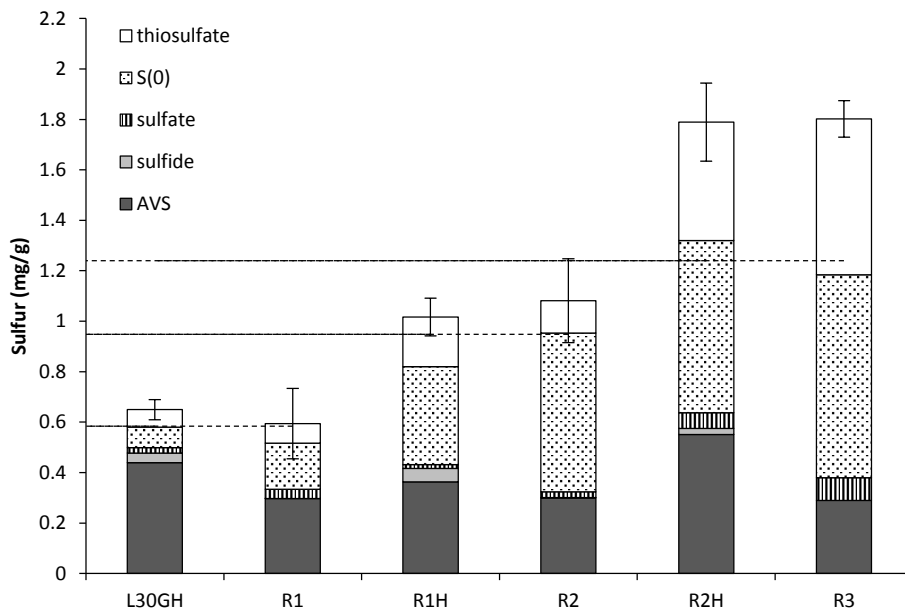
Fig. 4. SEM image of R3 to show the formation of elemental sulfur crystal and octahedral pyrite after reaction

414
415



416
417
418
419
420
421

Fig. 5. Influence of water content on sulfur product. Dotted lines represent H₂S input calculated from column tests. Error bars represent mean absolute deviation. Sulfur content in y-axis is expressed as mg of sulfur per 1 g of dry soil.

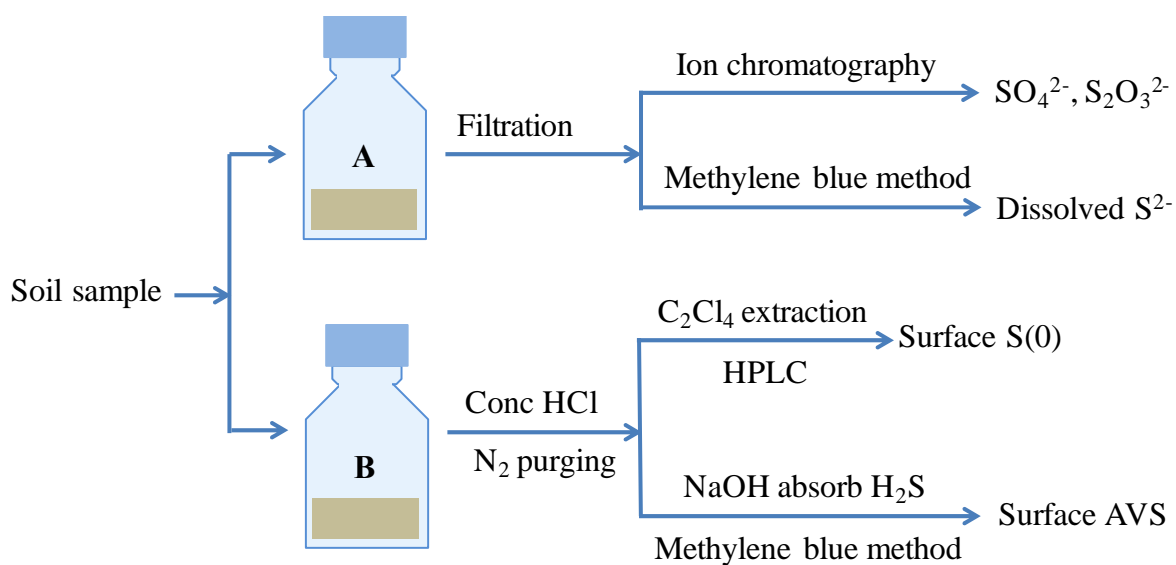


422
423
424
425
426

Fig. 6. Sulfur products in L30G regeneration and reuse. Dotted lines represent H₂S input calculated from column tests. Error bars represent mean absolute deviation. Sulfur content in y-axis is expressed as mg of sulfur per 1 g of bulk soil.

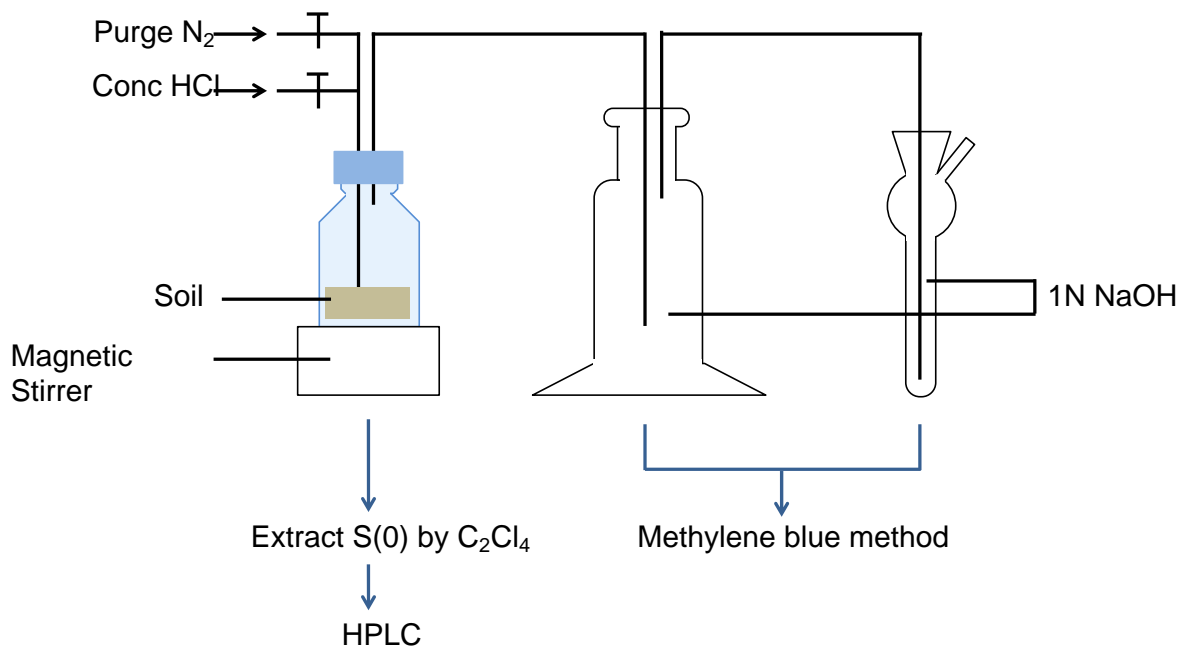
427
428
429
430

Supporting information



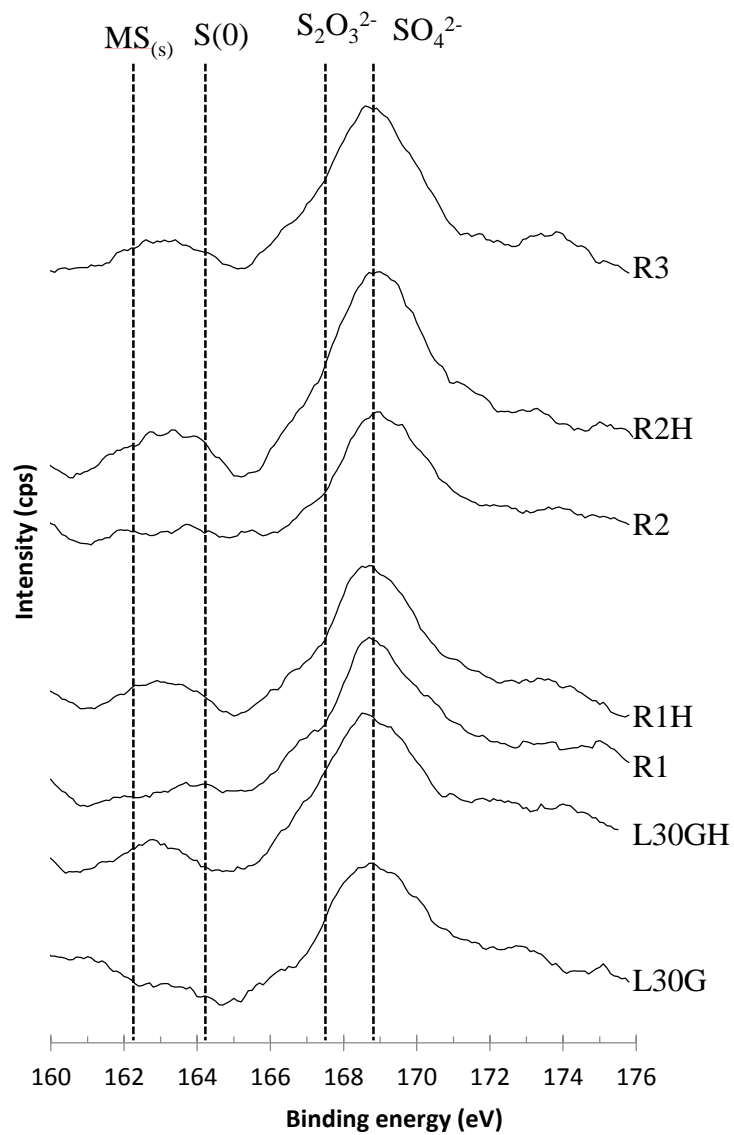
431
432
433
434
435
436
437

Fig. S1. Flow chart of chemical measurements



438

Fig. S2. Test setup for measurement of $\text{S}(0)$



439
 440
 441
 442

Fig. S3. XPS results of sulfur products in soil samples